Journal of Peptide Science
J. Peptide Sci. **5**: 32–45 (1999)

Construction and Synthesis of Lactoferricin Derivatives with Enhanced Antibacterial Activity

ØYSTEIN REKDAL[a], JILL ANDERSEN[b], LARS H. VORLAND[b] and JOHN S. SVENDSEN[c,*]

[a] Institute of Medical Biology, Faculty of Medicine, University of Tromsø, Tromsø, Norway
[b] Microbiology Department, University Hospital of Tromsø, Tromsø, Norway
[c] Department of Chemistry, Faculty of Science, University of Tromsø, Tromsø, Norway

Received 7 May 1998
Accepted 9 July 1998

Abstract: A series of peptides derived from sequences from human, bovine, murine and caprine lactoferrin has been prepared and investigated for antibacterial effect. Among the four species investigated peptides based on the bovine sequence displayed significant activity. The bovine sequence, bovine lactoferricin, showed a MIC value of 30 μg/mL on *E. coli* and *S. aureus*, whereas the three other lactoferricins possessed MIC values above 200 μg/mL. Based on these findings, novel peptides with enhanced antibacterial activities, were prepared with sequences designed by molecular modelling and structure-activity studies.

Keywords: lactoferricin; antibacterial; sequence modification; QSAR

INTRODUCTION

There is an increasing awareness that the highly specific cell-mediated immune system in vertebrates is supplemented with an innate non-specific immune system [1,2]. The innate immunity is provided by a chemical defence system where a series of distinct families of broad spectrum antibiotic peptides play a major role [3–7]. These peptides are closely related to antimicrobial peptides isolated from a variety of species including bacteria [8], insects [9,10], amphibians [11] and mammals [12]. In a majority of cases, antibiotic peptides have a net positive charge and a propensity to form amphiphilic α-helix or β-sheet structures upon interaction with the outer phospholipid bilayer in the bacterial cell membrane [13]. Although in most cases the detailed molecular mechanisms of the antibiotic action are still unknown, some of the peptides, class L (lytic) peptides [14], are believed to interact with bacterial cell membranes, probably forming ion-channels [15] or pores [16] leading to permeability changes and consequent cell lysis. The effect seems to be non-specific, and the different peptides bind in numbers suggesting highly repeated membrane components as possible target sites [17]. Synthetic enantiomers of cecropins and magainins preserve the antimicrobial effect, excluding a stereospecific recognition by receptors or enzymes [18]. The peptides show selectivity for prokaryotic and fungal cell membranes, a property probably linked to the high density of anionic phospholipids in their cell membranes [19]. Cholesterol which is present in eukaryotic cell membranes has been shown to stabilize artificial membranes and prevent membrane lysis by magainins and cecropins [20–23].

Lactoferrin is a part of the transferrin protein family which plays a key role in controlling the level of free iron in body fluids. In addition, lactoferrin

Abbreviations: ACM, acetamidomethyl; LFB, bovine lactoferricin; LFH, human lactoferricin; LFC, caprine lactoferricin; LFM, murine lactoferricin; QSAR, quantitative structure activity relationship; PLS, projection to latent structures.

* Correspondence to: Department of Chemistry, Faculty of Science, University of Tromsø, N-9037 Tromsø, Norway. E-mail: johns@chem.uit.no

CCC 1075–2617/99/050032-14$17.50

shows a weak antibacterial effect [24]. An antimicrobial peptide, much more effective than lactoferrin, is generated upon gastric pepsin cleavage of lactoferrin [24]. The active peptide of human lactoferrin, named lactoferricin H (LFH), and bovine lactoferrin, lactoferricin B (LFB), were isolated and sequenced [25] and identified as short fragments from, or close to, the N-terminus of lactoferrin. Although evolutionary unrelated with the antibiotic peptides from the non-specific immune system discussed above, LFB shares the highly cationic nature of class L peptides, and is found to be active against a wide range of Gram-negative and Gram-positive bacteria [26] and fungi [17]. LFB probably damage the outer membrane of Gram-negative bacteria [27], and it is thought that the main effect of LFB is to increase the permeability of the cytoplasmic membrane [26], closely resembling the mechanism of the class L antibiotic peptides.

Recently the amino acid sequence of murine [28] and caprine [29] lactoferrin have been determined, but their antibacterial effect are unknown. We have identified the lactoferricin regions in murine and caprine lactoferrin and prepared murine and caprine lactoferricin (LFM and LFC, respectively), as well as LFH and LFB, in order to investigate the structure-activity relationship of lactoferricins of human, bovine, murine and caprine origin. The antimicrobial activity of LFB have been improved by molecular modelling and rational design.

MATERIALS AND METHODS

MIC Tests

The bacterial strains used were: *Escherichia coli* ATCC 25922 and *Staphylococcus aureus* ATCC 25923. All strains were stored at -70°C. The bacteria were grown in 2% Bacto Peptone water (Difco 1807-17-4). All tests were performed with bacteria in mid-logarithmic growth phase. Determination of the minimum inhibitory concentration (MIC) of the peptides for bacterial strains were performed in 1% Bacto Peptone water. A standard microdilution technique with an inoculum of 2×10^6 cfu/mL was used. All assays were performed in triplets. Since the peptides are positively charged and henceforth could adhere to the plastic wells, the actual concentration of the peptides in the solution was controlled by HPLC. There was no difference between the concentration of the peptides before or after adding the solution to the plastic wells.

Molecular Modelling

The molecular modelling studies were performed using Macromodel 4.5, 5.0 and 6.0 [30] software on Silicon Graphics Personal Iris, Indy and O2 workstations. AMBER* force field with standard parameters, and a GB/SA water model were used in the calculations. Minimizations were performed with 5000 steps of Polak-Ribiere conjugated gradient. The dynamic simulations were performed using stochastic dynamics protocol at 300 K for 100–10000 ps using a time step of 1 fs.

Synthesis of Peptides

Initially, the lactoferricin B used was a gift from Wayne Bellamy (Nutritional Science Laboratory, Morinaga Milk Industry Co. Ltd, Kanagawa 228, Japan). Later in the study the peptides were synthesized with a 9050 Plus PepSynthesizer (Milligen). All peptides were synthesized on solid phase by use of fluorenylmethoxycarbonyl (Fmoc) chemistry. Cysteines in cystein containing peptides were protected with acetamidomethyl groups to prevent disulfide bridge formation. The peptides were analysed and purified by reversed phase HPLC on a Waters 600E chromatograph (Millipore) with UV detection at 254 nm. The fractions purified on HPLC were analysed on a liquid chromatography-mass spectrometer (LC-MS) with electrospray interface (Fisons VG Quattro) or/and with fast atom bombardment mass spectrometry (FAB-MS) (Fisons VG Tribrid).

Calculations

The hydrophobicity, H, of each peptide was calculated by summation of each residue hydrophobicity, H_n, using Eisenbergs normalized consensus scale [31]. The mean hydrophobicity is the average H_n of all residues in the peptide. For the calculation of the other peptide descriptors the DNA-star software package was used.

Multivariate Statistical Analysis

Multivariate statistical analysis was performed using SIMCA-S v5.1a software from Umetri AB, Umeå, Sweden.

RESULTS AND DISCUSSION

Structure of the Lactoferricins

The structure of human lactoferrin is determined to 2.8 and 2.2 Å resolution by X-ray crystallography

[32,33]. Human lactoferricin (LFH) consists of residues 1–47 of human lactoferrin. LFH contains two peptide fragments; one consisting of residues 12–47 cyclised with a disulfide bridge between Cys20 and Cys37, the second fragment (residues 1–11) is connected to the 12–47 fragment through a disulfide bridge between Cys10 and Cys46. In the human lactoferrin structure, the corresponding residues comprises a β-strand (residues 4–11), an α-helix (residues 12–29), a turn (residues 30 and 31), followed by a β-strand (residues 31–47) [34]. Bovine lactoferricin (LFB) with only 25 residues (residues 17–41) in a single chain is structurally much simpler than LFH. However, neither the N-terminal segment in LFH nor the presence of the disulfide bridge in LFH and LFB is reported to be necessary for the antibacterial activity [25]. Our results, however, indicate that some activity is lost by reduction of the disulfide bridge.

To gain insight into the structural properties of the lactoferricins, a molecular modelling study of human and bovine lactoferricins was performed. A simplified model peptide of human lactoferricin, LFH(12–47), where the N-terminal fragment (residues 1–11) was omitted, was used as a starting point for the modelling process. The coordinates for the non-hydrogen atoms in residues 12–47 were extracted from the Brookhaven protein data bank structure file of human lactoferrin. The structure was rectified by modifying the N- and C-termini and hydrogen atoms were added before minimization. As shown in Figure 1, the helix-turn-strand motif found in the intact protein was conserved in the minimized lactoferricin peptide. The minimized structure was then subjected to a stochastic dynamics simulation for 1000 ps. A stochastic simulation procedure was chosen, because a stochastic method explores the conformational space more efficiently than conventional molecular dynamics simulation. Even though a 1000 ps simulation of a peptide of this complexity cannot explore the conformational space in a convergent manner, the simulations clearly show that the conformation of the residues engaged in the helix-turn-strand motif was conserved during the simulation. Not unexpectedly the largest atomic motions were found in the peptide termini, especially in the end of the strand. The presence of helical structures could also be observed for a synthetic truncated LFH analog, LFH(18–42), in the far UV circular dichroism spectrum of the peptide dissolved in 25% 2,2,2-trifluoroethanol (TFE) in water.

The structure of bovine lactoferricin, LFB(17–41), was modelled based on the LFH(12–47) minimum energy conformation by substituting every side chain in the human structure with that of the bovine peptide. The starting structure was minimized (Figure 1) and subjected to a 1000 ps stochastic simulation at 300 K. The results obtained for LFB(17–41) resembled those of LFH(12–47), with the exception that the bovine peptide seemed to display less flexibility yielding an overall 'stiffer' structure. The common structural theme is still an α-helix, a turn and a β-strand in agreement with CD experiments on a synthetic LFB(17–41) peptide (in 25% TFE in water) with ACM protection of Cys19 and 36. After this modelling work was completed, the X-ray crystallographic structure of bovine lactoferrin (diiron form) at 2.8 Å resolution was reported [35]. The results obtained in our modelling process were in accordance with results from simulations starting from the crystallographic structure of bovine lactoferrin.

Antibiotic Activity of Synthetic Lactoferricins with Sequences from Different Species

The amino acid sequence of lactoferrins from goat [29] and mouse [28] have been determined and show high sequence homology with both the human and the bovine lactoferrins. The residues engaged in the helix-turn-strand motif can easily be identified in the sequence as shown in Table 1. As LFB is more antibacterial than LFH [25], the residues corresponding to LFB(17–41) were chosen in the amino acid sequence of human, murine and caprine lactoferrin to prepare analogous lactoferricin peptides; LFH(18–42), LFM(17–41) and LFC(17–41), respectively. The disulfide bridge is not essential for antibiotic activity in bovine and human lactoferricin [25] and all peptides were prepared with ACM protection of the cysteine residues to avoid cyclisation or oxidation.

The antibacterial activities of the synthetic lactoferricins expressed as MIC are compiled in Table 2 which shows that only LFB(17–41) displayed significant antibacterial activity against *E. coli* and *S. aureus*.

It has previously been reported that the efficiency of some antimicrobial peptides shows correlation with the net charge at neutral pH [36]. The calculated net charge of the peptides are compiled in Table 1, and it is interesting to note that the sole active peptide, LFB(17–41), has the highest net charge at pH 7. The correlation in our peptides is not very clear, LFC(17–41) with a net charge of 6.85 at neutral pH are nearly void of antimicrobial activity, however, the activity of the less charged peptides are even lower.

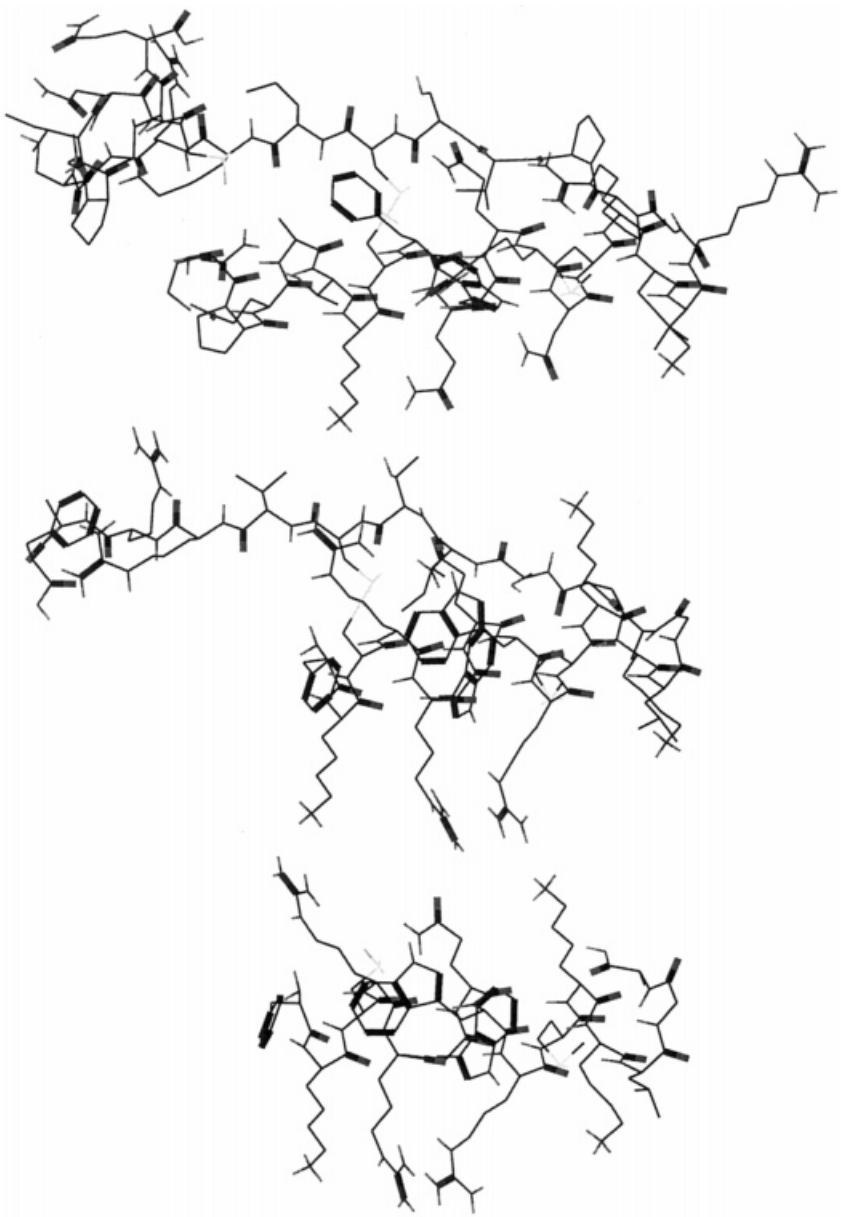

Figure 1 Plot of minimized conformations of LFH(18–42) (top), LFB(17–41) (middle) and LFB(17–31) (bottom).

LFB Analogs with Different Chain Length

Another important property determining the antibacterial activity of linear peptides is linked to their ability to adopt helical structures [37]. In the intact lactoferrin protein, residues 14–28 are located in an α-helix, residues 29–31 comprise a turn and residues 32–41 are in a β-strand. We therefore anticipated that the antibacterial effect of the lactoferricins could originate from the part of the sequence that participates in the helix of the intact protein. As the bovine lactoferricin sequence, LFB(17–41), was the only peptide with significant antibacterial property, we chose to prepare a shorter variety of the bovine peptide, LFB(17–31), containing both the helix and turn residues of the protein, while the ten residues encompassing the strand were removed (Table 1). Molecular modelling of LFB(17–31) showed that the helical structure is an energy minimum (Figure 1) and that the helix survived a 10000 ps stochastic dynamics simulation at 300 K, whereas the turn area seemed very

Table 1 Amino Acid Sequence, Charge at pH 7 and Molecular Mass for Synthetic Lactoferricins from Different Species

Species	Sequence	Name	Charge at pH 7	Molecular mass measured (calculated)
Human	T K C F Q W Q R N M R K V R G P P V S C I K R D S	FH(18–42)	5.85	3163.4[b] (3163.8)
Bovine	F K C R R W Q W R M K K L G A P S I T C V R R A F	LFB(17–41)	7.84	3267.2[b] (3268.2)
Murine	E K C L R W Q N E M R K V G G P P L S C V K K S S	LFM(17–41)	3.85	3003.2[b] (3003.7)
Caprine	S K C Y Q W Q R R M R K L G A P S I T C V R R T S	LFC(17–41)	6.85	3154.4[b] (3154.8)
Bovine	P E W F K C R R W Q W R M K K L G A	LFB(14–31)	6.85	2476 (2477.8)[b]
Bovine	F K C R R W Q W R M K K L G A	LFB(17–31)	5.88	2066 (2065.8)[a]
Bovine	K C R R W Q W R M K K L G A	LFB(18–31)	5.88	1916 (1917.6)[a]
Bovine	C R R W Q W R M K K L G A	LFB(19–31)	4.88	1791 (1789.4)[a]
Bovine	R R W Q W R M K K L G A	LFB(20–31)	4.91	1616 (1615.1)[a]
Bovine	K K C R R W Q W R M K K L G A	LFB(17–31)K17	6.87	2048 (2045.8)[a]
Bovine	F K C **F** R W Q W R M K K L G A	LFB(17–31)F20	5.87	2059 (2055.8)[a]
Bovine	**K** K C **F** R W Q W R M K K L G A	LFB(17–31)K17,F20	4.88	2039 (2036.8)[a]
Secondary structure	←−−−−Helix−−−−→ <Turn> ←−−−Sheet−−→			

[a] M determined by FAB MS.
[b] M+H determined by ESI MS.

flexible as shown in Figure 2. Despite that LFB(17–31) has a lower net charge (Table 1), than LFB(17–41) and LFC(17–41), it still retains most of the antibacterial effect as shown in Table 2. These findings indicate that even if the overall charge is important, it is not sufficient for antibacterial activity.

Several reports indicate that the antibiotic activity of different classes of linear peptides (e.g. magainins and defensins) is connected to their ability to adopt amphipathic α-helical structures [13,38–40]. A helical wheel representation [41] of the helix residues of LFB(17–31) is shown in Figure 3, but no clear amphipathy in the peptide is evident from this drawing with many polar residues flanking all sides of the helix. An uneven distribution of charged residues is however present, with four basic residues, Lys2 and 12 together with Arg5 and 9, located in one sector of the helix, whereas non-basic, but mainly polar, residues flank the rest of the helix. An exception are residues Arg4 and Lys11 which are located in the overall 'non-basic' area of the peptide. If an uneven distribution of charge is important, inspection of helical wheel representation of the corresponding helix residues in LFH(18–42), LFM(17–41) and LFC(17–41) clearly show that these peptides should be expected to display lower activity. None of these segments display the array of four basic residues flanking one face of the helix; the caprine and the murine peptide both have three basic residues together with one polar and one acidic residue, respectively. The human peptide has just two Lys in this array together with the two polar and neutral residues Gln and Asn. The antibiotic activity of these peptides are all very low; however, the caprine peptide is more active than the murine and human peptide as could be expected from the discussion above.

Table 2 Minimum Inhibitory Concentration (MIC) in μg/mL (μM) of Synthetic Lactoferricins on *E. coli* ATCC 25922 and *S. aureus* ATCC 25923

Peptide	*E. coli* ATCC 25922 MIC	*S. aureus* ATCC 25923 MIC
LFH(18–42)	>200	>200
LFB(17–41)	30	30
LFM(17–41)	>200	>200
LFC(17–41)	750	>1000
LFB(14–31)	70 (28)	>200 (80)
LFB(17–31)	40 (20)	100 (50)
LFB(18–31)	80 (43)	200 (108)
LFB(19–31)	200 (120)	>250 (150)
LFB(20–31)	100 (62)	200 (124)
LFB(17–31)K17	60 (30)	100 (50)
LFB(17–31)F20	20 (10)	200 (100)
LFB(17–31)K17,F20	20 (10)	200 (100)

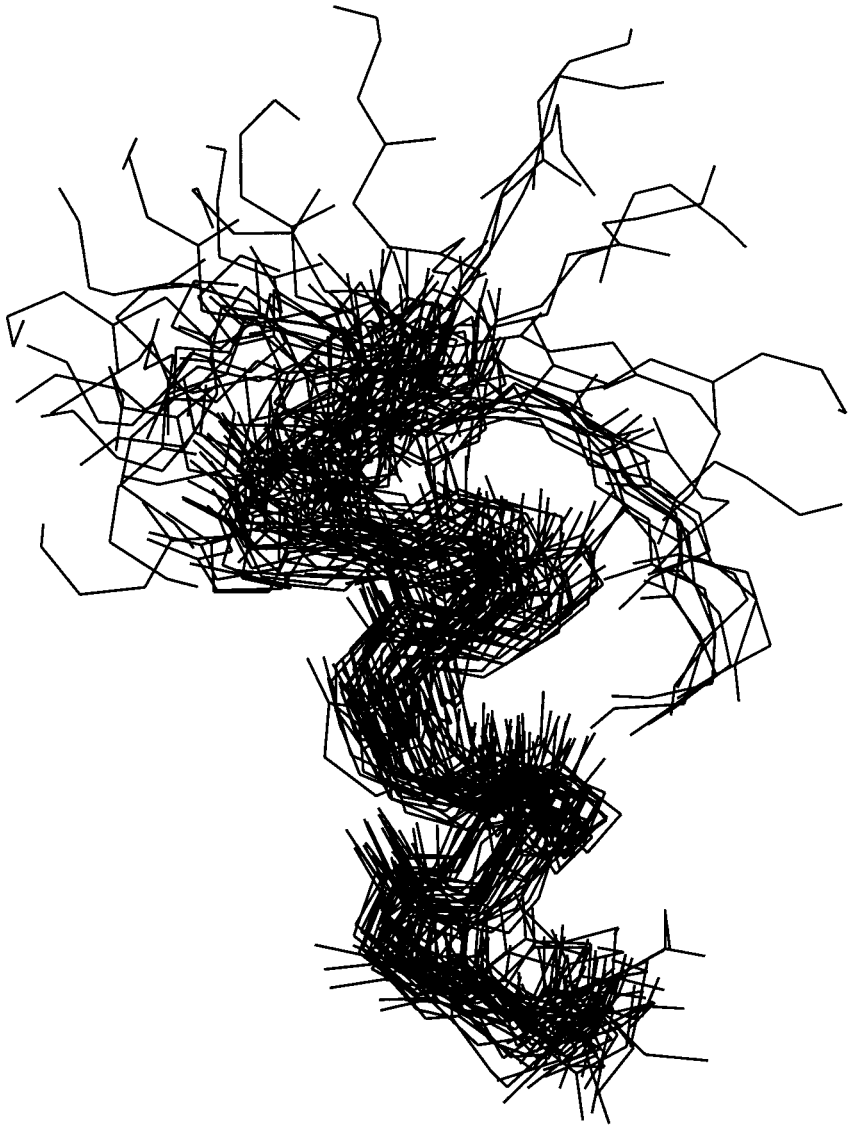

Figure 2 Peptide backbone overlay plot of 100 evenly sampled conformations of LFB(17–31) from a 10000 ps stochastic dynamics simulation at 300 K.

Helix 1 of bovine lactoferrin [34] has three more residues and hence one more turn than what is included in our LFB(17–31) peptide. We therefore prepared an extended peptide, LFB(14–31), including all amino acids necessary to complete helix 1 in the bovine lactoferrin protein (Table 1). The MIC value for *E. coli* of LFB(14–31) was higher than of LFB(17–31) as shown in Table 2. It was somewhat disappointing that the 18-residue long LFB(14–31) did not show an increased activity despite the fact that this peptide is closer to the 20 residues required to span the bacterial cell membrane as an α-helix [42]. However, an explanation could be that the LFB(14–31) still is too short to span the membrane and none of the new residues included (Pro, Glu and Trp) are basic (cationic) residues. One of the added residues is acidic and thus decreased the overall cationic nature of the peptide. Decreasing the peptide length from the 15-residue LFB(17–31) to the shorter peptides LFB(18–31), LFB(19–31) and LFB(20–31) reduced the antibacterial activity (Table 2). It is interesting to note that LFB(19–31) is

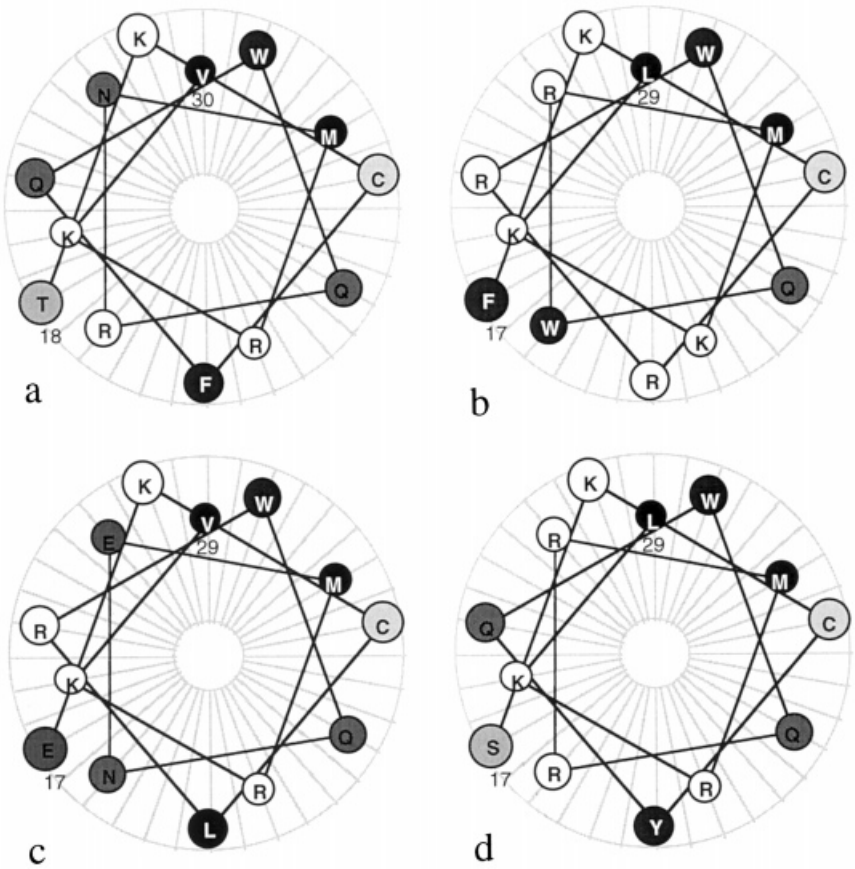

Figure 3 Edmundson helical wheel representation of the helix residues in (a) LFH(18–42), (b) LFB(17–41), (c) LFM(17–41) and (d) LFC(17–41).

the least potent peptide showing that the penalty of loosing one of the residues in the basic array, Lys18, is severe. More surprising is that the peptide with deletion of Cys19, LFB(20–31), gives an increased antibacterial activity compared to LFB(19–31). Recently, it has been reported that LFB(20–30) displays high activity against *E. coli* and *B. subtilis* [40].

Design of Enhanced Peptides Based on the Bovine Lactoferricin Sequence

As indicated from our results above, the presence of an array of four basic residues on one face of the lactoferricins appeared to be important for antibacterial efficiency. The peptide length of 15 residues clearly limits the possibility of improving the efficiency of LFB(17–31) by increasing the size of the array of basic residues. If on the other hand, the asymmetry in charge distribution is important, the distribution of the residues in LFB(17–31) is far from optimal with two cationic residues located in the 'non-cationic' sector and a lipophilic Phe in the cationic sector. There are at least two directions for increasing the charge asymmetry; increase the area (and the number of basic residues) or decrease the cationic charge in the neutral sector of the peptide. Three model peptides were designed to test this hypothesis; LFB(17–31)K17 which increases the number of basic residues in the cationic sector, LFB(17–31)F20 which increases both the lipophilicity and charge asymmetry while simultaneously decreasing the overall charge, and LFB(17–31)K17,F20 which seeks to address both issues simultaneously. Schiffer-Edmundson helical wheel representations of these peptides are shown in Figure 4. Table 2 shows the MIC values for these three sequence modified peptides. LFB(17–31)K17 was slightly less active than LFB(17–31) with an increased MIC against *E. coli*. The LFB(17–31)F20 peptide was significantly more active against *E. coli* with a decreased MIC value. The efficacy against *S. aureus* was, however, decreased. The doubly substi-

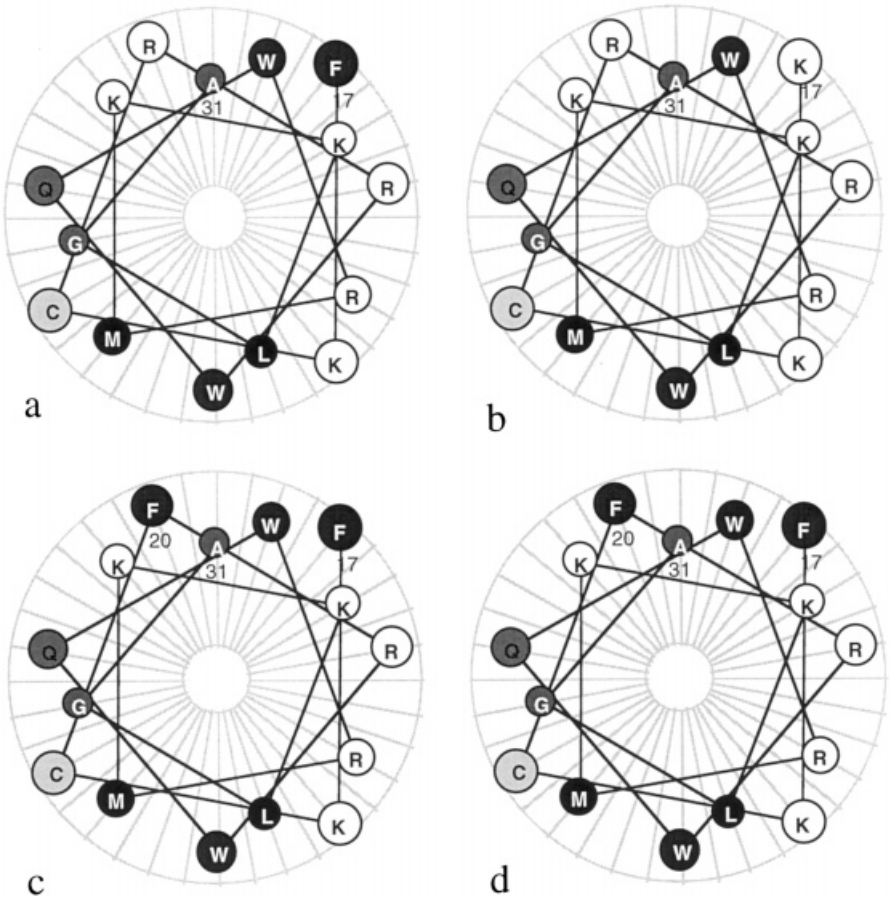

Figure 4 Edmundson helical wheel representation of (a) LFB(17–31), (b) LFB(17–31)K17, (c) LFB(17–31)F20 and (d) LFB(17–31)K17,F20.

tuted peptide LFB(17–31)K17,F20 displayed a similar effect as LFB(17–31)F20, indicating that the lipophilic substitution in the 'non-cationic' sector had the largest effect. These results indicate that increasing the cationic array on the LFB derivatives may not necessarily increase the activity; on the other hand, a significant increased activity should be possible by lipophilic modification of the non-basic part of the peptide.

QSAR Studies of the Lactoferricin Peptides

Until now, the present study of antibacterial activity of the synthetic peptides have pointed out several important properties an effective antibiotic lactoferricin peptide should possess; the chain length should not be shorter than 15 residues, while the net positive charge and the charge asymmetry should be large. The interplay between these, and possibly other factors have not yet been addressed. Classical multiple regression analysis on a small data set is generally not advisable, and we therefore subjected the eight bovine lactoferricin derivatives compiled in Table 3 to multivariate statistical analysis [43] using the SIMCA software system which can give robust statistical analysis with as little as five observations (peptides). We first chose the peptide descriptors we anticipated were important, e.g. chain length and net charge at pH 7. A problem occurred when finding a descriptor for charge asymmetry as no standard peptide descriptor handles this property explicitly. Amphipathy, which describes the degree of asymmetric distribution of hydrophobic and hydrophilic residues in a helical structure, could be connected to charge asymmetry. Amphipathy can be described by Eisenbergs hydrophobic moment [44], μ, and was calculated for each peptide using the following formula:

$$\mu = \left[\left(\sum_{n=1}^{N} H_n \sin(\delta n) \right)^2 + \left(\sum_{n=1}^{N} H_n \cos(\delta n) \right)^2 \right]^{1/2}$$

Table 3 Descriptors* Used in the Multivariate QSAR of the Lactoferricin Peptides

Peptide	*N*	*H*	Kyte–Doolittle *H*	*M*	μ	*C*	*X*	Garnier α	Chou–Fasman α	Emini surface probability
LFB(14–31)	18	−0.3806	2.82	0.2570	4.6264	0.1892	3.0453	0.404	0.374	1.02
LFB(17–31)	15	−0.4693	1.28	0.3216	4.8238	0.1749	2.6229	0.467	0.800	1.39
LFB(18–31)	14	−0.5879	1.40	0.4268	5.9756	0.1873	2.6229	0.500	0.857	1.50
LFB(19–31)	13	−0.3319	1.28	0.4680	6.0840	0.1966	2.5558	0.538	0.933	1.42
LFB(20–31)	12	−0.5850	1.37	0.4845	5.8140	0.2130	2.5558	0.583	1.000	1.70
LFB(17–31)K17	15	−0.6487	1.53	0.4963	7.4447	0.2370	3.5550	0.467	0.800	1.61
LFB(17–31)F20	15	−0.2213	1.09	0.3563	5.3447	0.1815	2.7224	0.533	1.000	1.17
LFB(17–31)K17,F20	15	−0.4007	1.09	0.4778	7.1213	0.2326	3.4886	0.533	1.000	1.07

* *H* is mean hydrophobicity, *M* is mean hydrophobic moment, μ is hydrophobic moment, *C* is mean charge moment, *X* is charge moment.

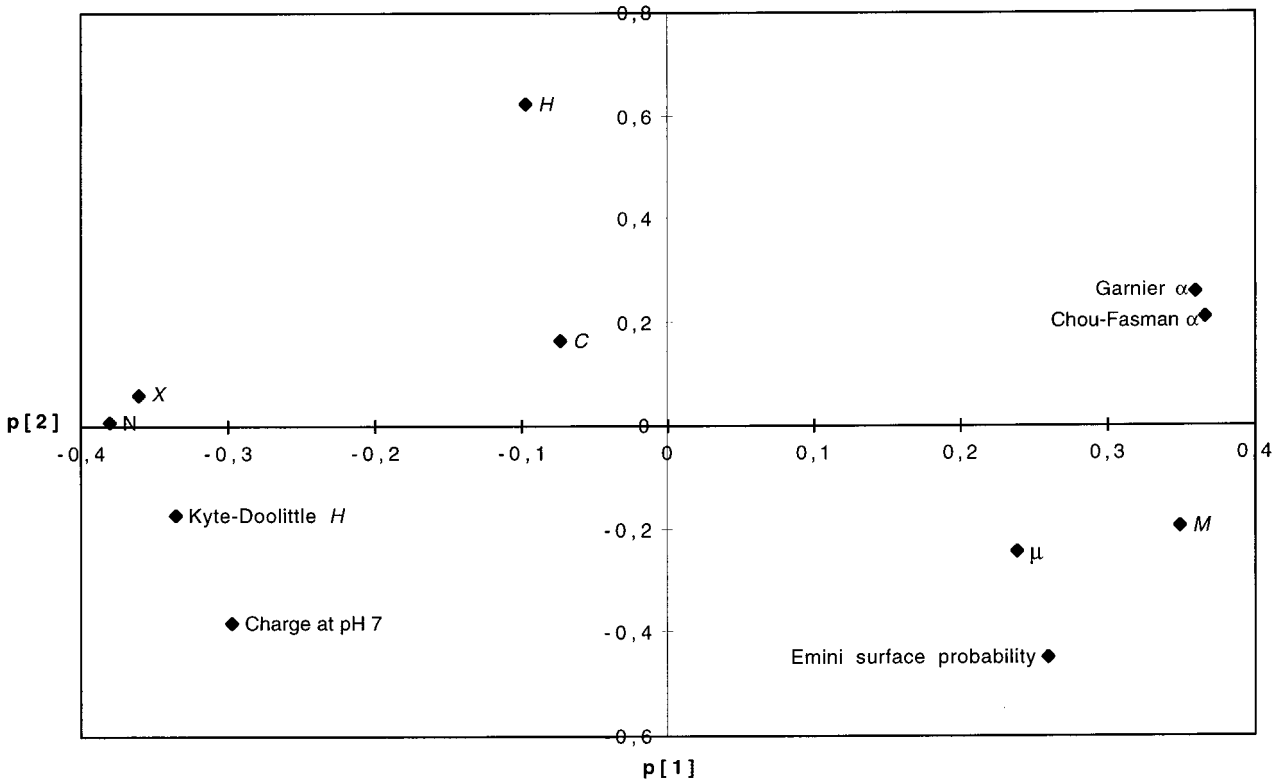

Figure 5 Scatter plot of the loadings in the principal components (PC) analysis of the 12 descriptors chosen for the synthetic bovine lactoferricin peptides in Table 3.

where H_n is the residue hydrophobicity [31] of the nth residue and $\delta = 100°$ assuming α-helical structures. The mean hydrophobicity, M, is defined:

$$M = \mu/N$$

where N is the number of residues in the peptide.

A new descriptor to describe charge asymmetry, charge moment, χ, is proposed and defined as follows:

$$\chi = \left[\left(\sum_{n=1}^{N} C_n \sin(\delta n) \right)^2 + \left(\sum_{n=1}^{N} C_n \cos(\delta n) \right)^2 \right]^{1/2}$$

where C_n is the normal charge of the amino acid side chain at pH 7. The C_n values are set to zero for all residues except lysine, arginine and histidine with $C_n = 1$ and aspartate and glutamate with $C_n = -1$. The descriptor χ will correlate positively with increasing asymmetry of charge distribution in an α-helix. The corresponding mean charge moment is defined as:

$$C = \chi/N$$

We also chose Eisenberg [31] and Kyte and Doolittle [45] hydrophobicity, Garnier [46] and Chou–Fasman [47] α-helix propensity and Emini surface probability as descriptors for different physical and structural properties of the peptides. All descriptors for the peptides are compiled in Tables 1 and 3.

First we performed a principal component (PC) analysis in the descriptor space for the eight peptides. In PC analysis, the orthogonal principal components are oriented such as they cover as much of the variation in the descriptors as possible. The PC analysis shows that 75% of the variation in the descriptors could be described by the two first principal components, p[1] and p[2]. Scatter plots of the loading of the different descriptors along the first and second principal components are shown in Figure 5, and reveal that the descriptors are well separated. Garnier and Chou–Fasman α-helix propensity are closely correlated in this data set, and for these peptides the calculated α-helicity is inversly correlated with Kyte–Doolittle hydrophobicity. The mean charge moment, C, have only a minor contribution to the first two principal components. A scatter plot of the scores in the two first principal components (Figure 6) show that the different peptides are sufficiently separated in the de-

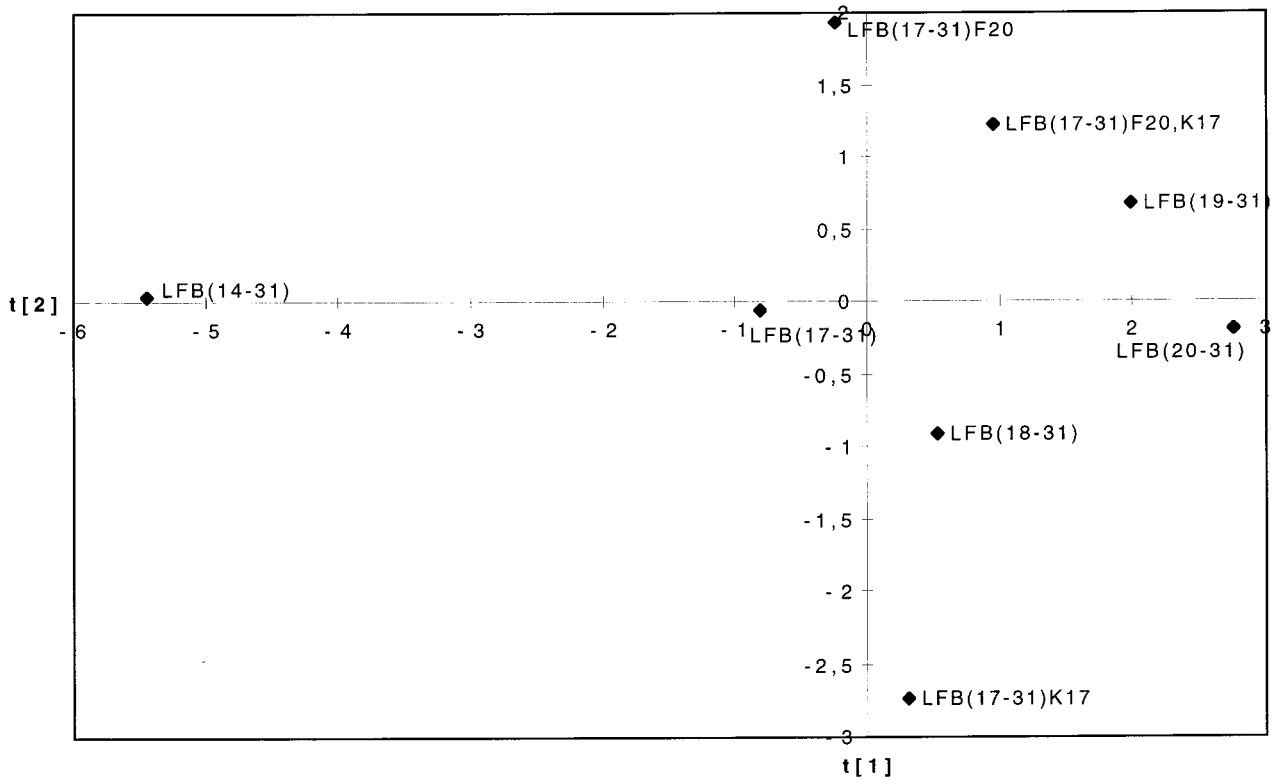

Figure 6 Scatter plot of the scores in principal components p[1] and p[2] of the synthetic bovine lactoferricin peptides in Table 3.

scriptor space; however, three clusters are apparent, the first consisting of LFB(17–31) F20, LFB(17–31) F20,K17, LFB(19–31) and LFB(20–31), the second LFB(17–31), LFB(18–31) and LFB(17–31) K17, and the last containing LFB(14–31). The latter peptide has a low score in p[1] and may be a candidate for an outlier along p[2].

The principal component analysis of the descriptor space has two objectives. The first is to reveal hidden or circumstantial correlations between the descriptors and thus insure that the descriptors chosen describe different properties in the peptides. The second objective is to control, that the model peptides chosen, really are different from the basic LFB(17–3l) sequence on the basis of the chosen descriptors. The PC analysis also has the capacity to cluster peptides with similar properties. The PC analysis does not link the peptides and their properties with their biological activity. Such information is available by projection to latent structures (PLS) modelling, where correlations between the peptide descriptors (the descriptor space) and the resulting biological activities (the resultant space) are revealed. In PLS modelling the principal components are chosen in a manner that covers the greatest variation in biological activities. The elements in the descriptor space are then connected to the orthogonal principal axes found in the resultant space. As in PC modelling, the importance of the different descriptors can be visualized as a scatter plot of the loading of each descriptor (property) on the principal axes. The orientation of the principal axes is, however, determined by the bioactivity, and the loading of each descriptor may therefore be different than in PC modelling. In addition, PLS analysis can also show the loadings of the bioactivity on the principal components. Such a combined p[1] + c[1] versus p[2] + c[2] scatter plot is shown in Figure 7 which reveals that the vectors connecting the loading in MIC for *E. coli* and *S. aureus* are close to orthogonal. This result shows that the peptide properties described in Table 3 have quite a different impact on the antibacterial activity against *E. coli* or *S. aureus*, and open the possibility to construct selective antibacterial peptides by making a judicious choice of which parameters should be changed. Combined scatter plots as shown in Figure 7 can operate as a visual aid in making the correct choices. Each of the points in the scatter plot can be regarded as end points of a vector originating in origo. As an increased antibac-

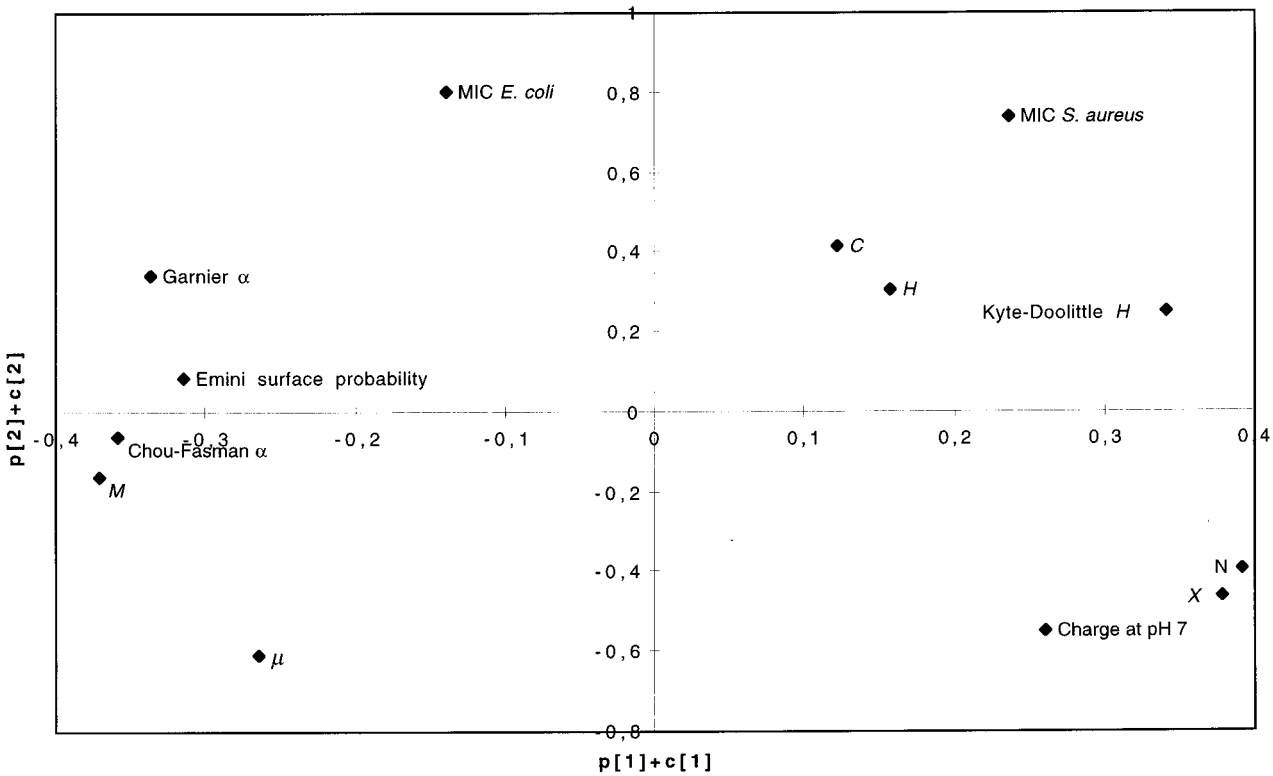

Figure 7 Combined scatter plot of the loadings in the PLS model of the antibacterial peptides in Table 3.

terial activity leads to a lower MIC, each peptide descriptor that has a negative component on the MIC vector will lower the corresponding MIC. For example, an increase in peptide charge at pH 7 will be expected to increase the antibacterial activity against *E. coli* because the peptide charge vector have a large negative component on the MIC *E. coli* vector. An increase in the number of residues and charge moment will also increase the activity against *E. coli*. Likewise, an increase in hydrophobic moment, μ, will lead to an increase in antibiotic activity against *S. aureus*. Because charge at pH 7 and μ are orthogonal to MIC *S. aureus* and MIC *E. coli*, respectively, peptides with alterations in these properties will be expected to increase their antibiotic selectivity for one of the bacterial strains.

CONCLUSIONS

We have in this study addressed the antibacterial activity of several lactoferricin analogs. By a combination of molecular modelling, peptide synthesis and quantitative structure activity relationship (QSAR) we have established that the antibacterial activity of the lactoferricins resides in the helix region of the peptide, and that, net charge, asymmetry in charge distribution and chain length are important factors for determining the antibiotic activity. We have also demonstrated that by changing these properties, the antibacterial efficiency as well as bacterial specificity of the lactoferricins can be altered. These findings point to important directions for the design and synthesis of novel lactoferricins with enhanced activity and a broader or a more specific antibacterial spectrum.

Acknowledgements

We gratefully acknowledge valuable discussions with Rolf Carlson and Morten Brændvang and research support from ALPHARMA AS and the Norwegian Research Council.

REFERENCES

1. A. Mor, K. Hani and P. Nicolas (1994). The vertebrate peptide antibiotics Dermaseptins have overlapping structural features but target specific microorganisms. *J. Biol. Chem. 269*, 31635–31641.
2. H.G. Boman (1996). Peptide antibiotics: holy or heretic grails of innate immunity? *Scand. J. Immunol. 43*, 475–482.
3. C.L. Bevins and M. Zasloff (1990). Peptides from frog skin. *Annu. Rev. Biochem. 59*, 395–414.
4. P. Nicolas and A. Mor (1995). Peptides an weapons against microorganisms in the chemical defence system of vertebrates. *Annu. Rev. Microbiol. 49*, 277–304.
5. R.I. Lehrer and T. Ganz (1996). Endogenous vertebrate antibiotics. *Ann. N. Y. Acad. Sci. 797*, 228–239.
6. J.A. Hoffmann and J.-M. Reichhart (1997). Drosophila immunity. *Trends Cell Biol. 7*, 309–316.
7. J. Nissen-Meyer and I.F. Nes (1997). Ribosomally synthesized antimicrobial peptides: their function, structure, biogenesis, and mechanism of action. *Arch. Microbiol. 167*, 67–77.
8. H.-G. Sahl in: *Gene-Encoded Antibiotics Made in Bacteria*, H.G. Boman, J. Marsh and J.A. Goode, Eds, p. 27–53, Wiley, New York, 1994.
9. H.G. Boman, I. Faye, G.H. Gudmundsson, J.-Y. Lee and D.-A. Lindholm (1991). Cell free immunity in Cecropia. A model system for antibacterial proteins. *Eur. J. Biochem. 201*, 23–31.
10. S. Cociancich, M. Goyffon, F. Bontems, P. Bulet, F. Bouet, A. Menez and J. Hoffmann (1993). Purification and characterization of a scorpion defensin, a 4 kDa antibacterial peptide presenting structural similarities with insect defensins and scorpion toxins. *Biochem. Biophys. Res. Commun. 194*, 17–22.
11. M. Zasloff (1987). Magainins, a class of antimicrobial peptides from Xenopus skin: isolation, characterization of two active forms, and partial cDNA sequence of a precursor. *Proc. Natl. Acad. Sci. USA 84*, 5449–5453.
12. R.I. Lehrer, A.K. Lichtenstein and T. Ganz (1993). Defensins: antimicrobial and cytotoxic peptides of mammalian cells. *Annu. Rev. Immunol. 11*, 105–128.
13. R. Besalle, A. Gorea, I. Shalit, J.W. Metzger, C. Dass, D.M. Desiderio and M. Fridkin (1993). Structure-function studies of amphiphilic antibacterial peptides. *J. Med. Chem. 36*, 1203–1209.
14. J.P. Segrest, H. DeLoof, J.G. Dohlman, C.G. Brouillette and G.M. Anantharamaiah (1990). Amphipatic helix motif: classes and properties. *Proteins 8*, 103–117.
15. K. He, S.J. Ludtke, W.T. Heller and H.W. Huang (1996). Mechanism of alamethicin insertion into lipid bilayers. *Biophys. J. 71*, 2669–2679.
16. S.J. Ludtke, K. He, W.T. Heller, T.A. Harroun, L. Yang and H.W. Huang (1996). Membrane pores induced by magainin. *Biochemistry 35*, 13723–13728.
17. W. Bellamy, H. Wakabayashi, M. Takase, K. Kawase, S. Shimamura and M. Tomita (1993). Killing of *Candida albicans* by lactoferricin B, a potent antimicrobial peptide derived from the N-terminal region of bovine lactoferrin. *Med. Microbiol. Immunol. 182*, 97–105.
18. D. Wade, A. Boman, B. Wahlin, C.M. Drain, D. Andreu, H.G. Boman and R.B. Merrifield (1990). All D-amino acid containing channel forming antibiotic peptides. *Proc. Natl. Acad. Sci. USA 87*, 4761–4765.
19. I.V. Polozov, A.I. Polozova, E.M. Tytler, G.M. Anantharamaiah, J.P. Segrest, G.A. Woolley and R.M. Epand (1997). Role of lipids in the permeabilization of membranes by class L amphipatic helical peptides. *Biochemistry 36*, 9237–9245.
20. Y. Nakajima, X.-M. Qu and S. Natori (1987). Interaction between liposomes and sarcotoxin IA, a potent antibacterial protein of *Sarcophaga peregrine* (flesh fly). *J. Biol. Chem. 262*, 1665–1669.
21. B. Christensen, J. Fink, R.B. Merrifield and D. Mauzerall (1988). Channel-forming properties of cecropins and related model compounds incorporated into planar lipid membranes. *Proc. Natl. Acad. Sci. USA 85*, 5072–5076.
22. M. Jackson, H.H. Mantsch and J.H. Spencer (1992). Conformation of magainin-2 and related peptides in aqueous solution and membrane environments probed by Fourier transform infrared spectroscopy. *Biochemistry 31*, 7289–7293.
23. E.M. Tytler, G.M. Anantharamaiah, D.E. Walker, V.K. Mishra, M.N. Palgunachari and J.P. Segrest (1995). Molecular basis for procaryotic specificity of magainin-induced lysis. *Biochemistry 34*, 4393–4401.
24. M. Tomita, W. Bellamy, M. Takase, K. Yamauchi, H. Wakabayashi and K. Kwase (1991). Potent antibacterial peptides generated by pepsin digestion of bovine lactoferrin. *J. Dairy Sci. 74*, 4137–4142.
25. W. Bellamy, M. Takase, K. Yamauchi, H. Wakabayashi, K. Kawase and M. Tomita (1992). Identification of the bactericidal domain of lactoferrin. *Biochem. Biophys. Acta 1121*, 130–136.
26. W. Bellamy, M. Takase, H. Wakabayashi, K. Kawase and M. Tomita (1992). Antibacterial spectrum of lactoferricin B, a potent bactericidal peptide derived from the N-terminal region of bovine lactoferrin. *J. Appl. Bacteriol. 73*, 472–479.
27. K. Yamauchi, M. Tomita, T.J. Giehl and R.T. Ellison (1993). Antibacterial activity of lactoferrin and a pepsin-derived lactoferrin peptide fragment. *Infect. Immun. 61*, 719–728.
28. B.T. Pentecost and C.T. Teng (1987). Lactotransferrin is the major estrogen inducible protein of mouse uterine secretions. *J. Biol. Chem. 262*, 10134–10139.
29. F.L. Provost, M. Nocart, G. Guerin and P. Martin (1994). Characterization of the goat lactoferrin cDNA: assignment of the relevant locus to bovine U12 synteny group. *Biochem. Biophys. Res. Commun. 203*, 1324–1332.
30. F. Mohamadi, N.G.J. Richards, W.C. Guida, R. Liskamp, M. Lipton, C. Caufield, G. Chang, T. Hen-

drickson and W.C. Still (1990). MacroModel—An integrated software system for modeling organic and bioorganic molecules using molecular mechanics. *J. Comput. Chem. 11*, 440.

31. D. Eisenberg, R.M. Weiss, T.C. Terwilliger and W. Wilcox (1982). Hydrophobic moments and protein structure. *Faraday Symp. Chem. Soc. 17*, 109–120.
32. M. Haridas, B.F. Anderson and E.N. Baker (1995). Structure of human diferric lactoferrin refined at 2.2 Å resolution. *Acta Cryst. D51*, 629–646.
33. B.F. Anderson, H.M. Baker, G.E. Norris, D.W. Rice and E.N. Baker (1989). Structure of human lactoferrin: crystallographic structure analysis and refinement at 2.8 Å resolution. *J. Mol. Biol. 209*, 711–734.
34. C.L. Day, B.F. Anderson, J.W. Tweedie and E.N. Baker (1993). Structure of recombinant N-terminal lobe of human lactoferrin at 2.0 Å resolution. *J. Mol. Biol. 232*, 1084–1100.
35. S.A. Moore, B.F. Anderson, C.R. Groom, M. Haridas and E.N. Baker (1997). Three-dimensional structure of difeeric bovine lactroferrin at 2.8 Å resolution. *J. Mol. Biol. 274*, 222–236.
36. R.E.W. Hancock, T. Falla and M. Brown (1995). Cationic bactericidal peptides. *Adv. Microb. Phys. 37*, 135–175.
37. H.C. Chen, J.H. Brown, J.L. Morell and C.M. Huang (1988). Synthetic magainin analogoues with improved antimicrobial activity. *FEBS Lett. 236*, 462–466.
38. S. Lee, H. Mihara, H. Aoyagi, T. Kato, N. Izumiya and N. Yamasaki (1986). Relationship between antimicrobial activity and amphiphilic property of basic model peptides. *Biochim. Biophys. Acta 862*, 211–219.
39. A.E. Blondelle and R.A. Houghten (1992). Design of model amphipatic peptides having potent antimicrobial activities. *Biochemistry 31*, 12688–12694.
40. J.H. Kang, M.K. Lee, K.L. Kim and K.-S. Hahm (1996). Structure-biological activity relationships of 11-residue highly basic peptide segment of bovine lactoferrin. *Int. J. Peptide Protein Res. 48*, 357–363.
41. M. Schiffer and A.B. Edmundson (1967). Use of helical wheels to represent the structures of proteins and to identify segments with helical potential. *Biophys. J. 7*, 121–135.
42. J.D. Lear, Z.R. Wasserman and W.F. DeGrado (1988). Synthetic amphiphilic peptide models for protein ion channels. *Science 240*, 1177–1181.
43. R. Carlson. *Design and Optimization in Organic Synthesis*, Elsevier, Amsterdam, 1992.
44. D. Eisenberg, E. Schwarz, M. Komaromy and R. Wall (1984). Analysis of membrane and surface protein sequences with the hydrophobic moment plot. *J. Mol. Biol. 179*, 125–142.
45. J. Kyte and R.F. Doolittle (1982). A simple method for displaying the hydrophatic character of a protein. *J. Mol. Biol. 157*, 105–132.
46. J. Garnier, D.J. Osguthorpe and B. Robson (1978). Analysis of the accuracy and implication of simple methods for predicting the secondary structure of globular proteins. *J. Mol. Biol. 120*, 97–120.
47. P.Y. Chou and G.D. Fasman (1974). Prediction of protein conformation. *Biochemistry 13*, 222–245.

